A Multi-Factor Battery Cycle Life Prediction Methodology for Optimal Battery Management

Valentin Muenzel*
Electrical and Electronic Eng.
University of Melbourne
Victoria, Australia

Julian de Hoog
IBM Research - Australia
Victoria, Australia

Marcus Brazil
Electrical and Electronic Eng.
University of Melbourne
Victoria, Australia

Arun Vishwanath
IBM Research - Australia
Victoria, Australia

Shiv. Kalyanaraman
IBM Research - Australia
Victoria, Australia

ABSTRACT

Affordability of battery energy storage critically depends on low capital cost and high lifespan. Estimating battery lifespan, and optimising battery management to increase it, is difficult given the associated complex, multi-factor ageing process. In this paper we present a battery life prediction methodology tailored towards operational optimisation of battery management. The methodology is able to consider a multitude of dynamically changing cycling parameters. For lithium-ion (Li-ion) cells, the methodology has been tailored to consider five operational factors: charging and discharging currents, minimum and maximum cycling limits, and operating temperature. These are captured within four independent models, which are tuned using experimental battery data. Incorporation of dynamically changing factors is done using rainflow counting and discretisation. The resulting methodology is designed for solving optimal battery operation problems.

Implementation of the methodology is presented for two case studies: a smartphone battery, and a household with battery storage alongside solar generation. For a smartphone that charges daily, our analysis finds that the battery life can be more than doubled if the maximum charging limit is chosen strategically. And for the battery supporting domestic solar, it is found that the impact of large daily cycling outweighs that of small more frequent cycles. This suggests that stationary Li-ion batteries may be well suited to provide ancillary services as a secondary function.

The developed methodology and demonstrated use cases represent a key step towards maximising the cost-benefit of Li-ion batteries for any given application.

*Please address all correspondence to this author at v.muenzel (at) student.unimelb.edu.au

e-Energy'15, July 14–17, 2015, Bangalore, India.

ACM: 978-1-4503-3609-3/15/07 . . . $15.00
DOI: http://dx.doi.org/10.1145/2768510.2768532.

Keywords

Lithium-ion (Li-ion) batteries; cell degradation; cycle life prediction; battery value optimisation

1. INTRODUCTION

There is a growing need for affordable decentralised energy storage. The market for energy storage is predicted to grow by 50% in the six years to 2020 [7]. Rechargeable batteries, including lithium-ion, are promising candidates given their rapidly decreasing cost [10].

Rechargeable lithium-ion (Li-ion) batteries have been used in laptop computers, mobile phones, and other portable electronic devices since the 1990s. More recently, they are being implemented in much larger applications. These include hybrid-electric and pure electric vehicles, as well as stationary energy storage for domestic, industrial, and power grid-support applications. This transition to larger applications is not straightforward. The low power draw of portable electronics limits heat generation in battery cells, thereby facilitating battery management. Low power also means a low storage voltage is acceptable, allowing only one or a few cells to be used, which require only a very simple battery management system. Also, portable electronics are typically designed for a lifespan of three years or less.

Conversely, large battery systems typically have a large power draw, requiring a multitude of cells, as well as more complex battery and thermal management systems. They have significantly longer lifetimes, in many cases of more than ten years. And the high initial investment involved means that battery systems become strategic assets and the lifetime preservation is of critical importance.

Managing batteries for longer lifetimes, however, is not straightforward. In the literature, few long-term experiments lasting five or more years have been published [1]. Of these, many were based on early battery chemistries, since which point significant progress has been made [15]. Concurrently, estimation methods of battery cycle life remain a field with ample scope for improvement.

The battery cycle life prediction methodologies developed to date can be divided into electrochemical and empirical approaches. Electrochemical cycle life prediction uses physically-based models alongside chemical reaction equations [2]. This is fundamentally the most accurate and insightful modelling approach as it captures physical and chemical characteristics

as part of the model. However, the vast number of physical and chemical parameters make fitting such models to any given cell a quite complicated and time-consuming process. This inhibits widespread use of such models.

Empirical approaches on the other hand use curve fitting to find general equations from discrete cycling measurement points. This reduces the complexity of model tuning notably. However, most empirical approaches focus on certain cells under a given range of conditions that entail only specific considered impact factors. This is done to limit the required amount of data and associated testing to a feasible volume. Ecker et al., for example, developed a life prediction model for pouch cells taking into account state-of-charge and temperature, but not charging or discharging currents [3]. And Ng et al. considered temperature, discharge current and depths-of-discharge, but does not consider charging currents or variations in the maximum state-of-charge [11].

The most encompassing empirically-based methodology, to the knowledge of the authors, was published by Omar et al. [13]. Their methodology uses separate models for four impact factors, all of which are modelled as independent from one-another. However, their methodology representing the state-of-the-art has room for improvement in several areas:

- It considers that for each cycle charging ends and discharging begins at 100% SOC. This may frequently be undesirable as high SOCs can lead to notable degradation during both cycling [4] and storage [3].
- Our attempts at replication found depth-of-discharge parameters that vary by several orders of magnitude from those published.
- The method of combining the various individual parameter models into a full model was demonstrated but not explained. It is based on fuzzy logic but is protected knowledge that the authors are not able to share (personal correspondence).
- The existing approach only predicts cycle life under static cycling conditions, in which cycling parameters such as currents and charging and discharging bounds do not change from cycle-to-cycle.

In this paper we present a battery life prediction model that addresses the above issues and is tailored towards usability as part of a battery management optimisation scheme. We make three main contributions to the literature:

1. We develop and demonstrate an empirically-supported model of how battery cycle life varies with interdependent average state-of-charge and depth-of-discharge[1].
2. We present a reproducible framework for combining numerous independent cycle life models considering different impact factors into a unified multi-factor cycle life model.
3. We develop and demonstrate a technique for enabling battery life prediction models to assess battery usage with dynamically changing cycling parameters.

We believe that the resulting model holds significant value for battery management and control optimisation for academic and commercial purposes alike.

[1]An explanation of domain-specific terminology is provided in Table 1.

Table 1: Domain-Specific Terminology

Notation	Meaning
CL	Cycle life; the number of cycles under certain conditions until the battery reaches its end-of-life of typically 70-80% of initial capacity.
DOD	Depth-of-discharge; the difference between minimum and maximum state-of-charge of a cycle.
nCL	Normalised cycle life; the cycle life of a battery under particular conditions divided by the cycle life under nominal conditions.
SOC	State-of-charge; the amount of charge stored in a battery at a given point of time divided by its nominal capacity. For the purpose of this paper we assume the battery voltage is fixed and the charge stored is directly proportional to energy stored.
SOC_{av}	Average state-of-charge; the mean of the maximum and minimum state-of-charge of a cycle.
SOC_{min}	The minimum state-of-charge reached during a given battery charge and discharge cycle.
SOC_{max}	The minimum state-of-charge reached during a given battery charge and discharge cycle.

2. METHODOLOGY

This section presents the combined cycle life algorithm, with following sections describing models for individual ageing factors for Li-ion batteries.

While the underlying methodology is valid for battery cells of any chemistry, the individual factor models and curve fitting are chemistry-dependent. The limited availability of suitable published Li-ion cell ageing data at present restricts us to taking a chemistry-agnostic approach here, but in future work this model is to be adjusted for specific Li-ion chemistries.

At the heart of the chosen approach, and as suggested in [13], is the assumption that the impacts that certain environmental and operational factors on lithium-ion battery cycle life are, or can be approximated as being, independent from one-another. Based on this independence assumption, it follows:

$$\frac{CL(x_1,...x_k)}{CL(x_{1,nom},...,x_{k,nom})} = \frac{CL(x_1)}{CL(x_{1,nom})} \times \cdots \times \frac{CL(x_k)}{CL(x_{k,nom})} \quad (1)$$

where CL is the predicted cycle life to a certain limit of degradation under given cycling parameters, x_k is the kth cycling parameter, and degradation impact factor, to be considered. In the case of interdependent ageing factors, the relevant factors need to be jointly included in one fraction on the right hand side. The index nom refers to nominal cycle life and cycling parameters, as found for example in a battery data sheet or gained from a cycling experiment for a single set of cycling parameters.

$$CL(x_1 \cdots x_k) = CL(x_{1,nom} \cdots x_{k,nom}) \times \frac{CL(x_1)}{CL(x_{1,nom})} \times \cdots \times \frac{CL(x_k)}{CL(x_{k,nom})} \quad (2)$$

In the case of lithium-ion battery ageing, among the most important impact factors are the operating temperature T, charging current I_{ch}, the discharging current I_d, as well as the minimum and maximum state-of-charge boundaries [4]. The following sections discuss and describe the development of impact factor models for these factors. The state-of-charge boundaries are transformed into depth-of-discharge DOD and average state-of-charge SOC_{av}.

The combined lithium-ion battery life cycle model, used in latter analysis and case studies, is formed by taking the product of the normalised individual models (Eqns. (7), (8, 9), and (18)) and the nominal cycle life:

$$CL(T, I_d, I_{ch}, SOC_{av}, DOD) = CL_{nom} \times nCL(T) \times nCL(I_d) \times nCL(I_{ch}) \times nCL(SOC_{av}, DOD) \quad (3)$$

where nCL is each associated normalised cycle life fraction, corresponding to terms on the right side of Eq. (1). This provides the underlying framework for predicting the cycle life of a given battery cell based on a single data cycle life data point. This data point can either come from manufacturer specifications, or from testing of a cell under a single set of cycling conditions.

2.1 Battery Currents and Temperature

For charging current, discharging current and working temperature of the cell, modified versions of the model published in [13] are used. In this model, cycle life is captured as a third order polynomial function of temperature:

$$CL(T) = aT^3 - bT^2 + cT + d \quad (4)$$

where a, b, c, and d are coefficients from fitting of experimental data on lithium iron phosphate based cells with values shown in Table 2. Note that the experiments in [13] used short-term cycling rather than as a simple constant current discharge, which is assumed here to have negligible impact.

The published model further approximates cycle life as a second-order exponential function of both discharging and charging current, respectively given as:

$$CL(I_d) = e \times exp(fI_d) + g \times exp(hI_d) \quad (5)$$

$$CL(I_{ch}) = m \times exp(nI_{ch}) + o \times exp(pI_{ch}) \quad (6)$$

where I_d and I_{ch} are the discharging and charging current, respectively, and e, f, g, h, m, n, o, and p are fit coefficients, the values of which are also listed in Table 2.

Eq. (3) requires each of the published models to be normalised. This normalisation is done as follows:

$$nCL(T) = \frac{aT^3 - bT^2 + cT + d}{aT_{nom}^3 - bT_{nom}^2 + cT_{nom} + d} \quad (7)$$

$$nCL(I_d) = \frac{e \times exp(fI_d) + g \times exp(hI_d)}{e \times exp(fI_{d,nom}) + g \times exp(hI_{d,nom})} \quad (8)$$

$$nCL(I_{ch}) = \frac{m \times exp(nI_{ch}) + o \times exp(pI_{ch})}{m \times exp(nI_{ch,nom}) + o \times exp(pI_{ch,nom})} \quad (9)$$

where nCL represents the normalised cycle life for each respective impact factor, T_{nom}, $I_{d,nom}$, and $I_{ch,nom}$, are nominal working temperature, nominal discharging current, and nominal charging current, respectively, as specified by the manufacturer for a given specified cycle life.

2.2 State-of-Charge and Depth-of-Discharge

By the nature of the coupling between the average state-of-charge, SOC_{av}, and depth-of-discharge, DOD, the respective impacts on cycle life are intuitively likely to be notably interdependent. For example, assume the life of a battery cell cycling between 40-60% (i.e. $SOC_{av} = 50\%$, and $DOD = 20\%$) is double that of a cell cycling from 30-70% ($SOC_{av} = 50\%$, and $DOD = 40\%$). This does not necessarily mean that a cell cycling between 10-30% SOC ($SOC_{av} = 20\%$, and $DOD = 20\%$) also has double the life of a cell cycling between 0-40% ($SOC_{av} = 20\%$, and $DOD = 40\%$). In fact, this is unlikely to give similar ageing, as discussed subsequently.

As a result an experimental dataset is required, in which both DOD and SOC_{av} are varied independently. Such a dataset was recently published by Ecker et al. [4]. It contains cycle life measurements for average SOC and DOD ranging from 10-90% and 10-100%, respectively. Obviously, the closer SOC_{av} is to either 0 or 100%, the lower the maximum DOD can be (a cell with an SOC_{av} of 10% can have at most a DOD of 20%, corresponding to cycling between 0-20% SOC).

Once digitised, a suitable fitting function is required for the dataset. [4] indicates that the cycle life of batteries decreases for cycling in both high and low SOC regions, while in mid-SOC regions less degradation occurs. This suggests a second-order polynomial function related to average SOC as a potentially suitable approach. The data further illustrates that as DOD increases, the cycle life reduces non-linearly. Having incorporated SOC_{av} as a second-order polynomial, a logical approach is to incorporate DOD as a multi-order polynomial also. Given the DOD and SOC_{av} are expected to be interdependent as discussed previously, there will also be one or more terms containing both variables.

Taking a second-order approach for DOD and SOC_{av}, the function to be fitted becomes:

$$CL^*(DOD, SOC_{av}) = q_0 + r_0 * DOD + s_0 * SOC_{av} + t_0 * DOD^2 + u_0 * DOD * SOC_{av} + v_0 * SOC_{av}^2 \quad (10)$$

where CL^* is the equivalent cycle life, and SOC_{av} and DOD are the average state-of-charge and depth-of-discharge over each cycle, respectively. Constants q_0, r_0, s_0, t_0, u_0, and v_0 are the fit coefficients. Curve fitting using the least-squares fitting method via the Matlab Curve Fitting Tool found these coefficients to have the values listed in Table 2.

As shown in left and centre of Fig. 1, this leads to a reasonably good fit, characterised by R-square and Root Mean Square Error values of 0.767 and 1220, respectively. Note that the figure shows all of the curve within the SOC_{av} and DOD range for which the cycle life is positive, including infeasible combinations of DOD and SOC_{av}. However, the fit has one problematic aspect. As shown in Fig. 1c, the maximum equivalent cycle life over SOC_{av} actually increases slightly when increasing DOD from around 85% upwards. This goes against the trend seen in experiments (e.g. [4]). A

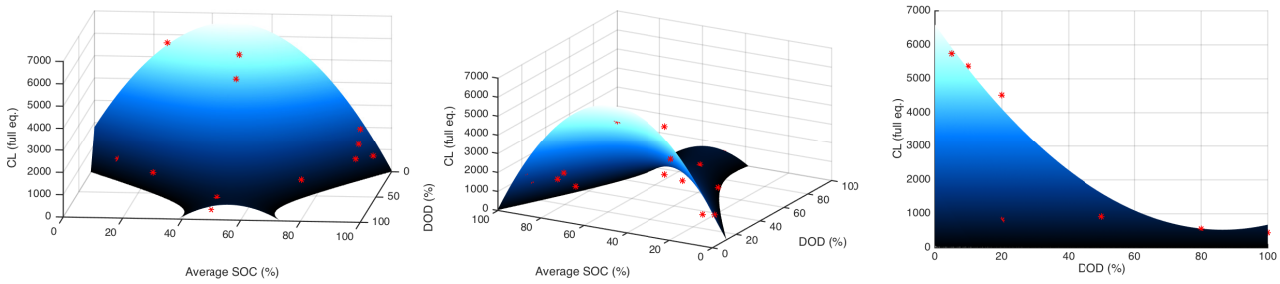

Figure 1: Two-variable second-order polynomial fit of cycle life as a function of average SOC and DOD. Figure on far right shows local minimum at $DOD < 100\%$, which is not consistent with practical findings.

Table 2: Values for tuning coefficients of models of lithium-ion degradation impact factors. Values for coefficients a$\cdots$p are as published in [13]. Coefficients $q_0 \cdots v_0$, and $q \cdots v$ are deduced in Section 2.2.

Variable	a	b	c	d	e	f	g	h	m	n	o	p
Value	0.0039	1.95	67.51	2070	4464	-0.1382	-1519	-0.4305	5963	-0.6531	321.4	0.03168
Variable	q_0	r_0	s_0	t_0	u_0	v_0	q	s	t	u	v	
Value	1806	-160.8	207.7	0.7901	0.4425	-2.250	1471	214.3	0.6111	0.3369	-2.295	

local maximum at the 100% DOD boundary is problematic for use in optimisation of battery management as it would encourage batteries to be cycled to its maximum limits, leading in practice to particularly strong degradation.

One approach to avoid this is to force the cycle life to have its minimum over DOD at 100% DOD at all SOC_{av} points. However, doing so removes the expected interdependency between SOC_{av} and DOD.

A different approach is to specify that the minimum only falls on a specific single point where $DOD = 100\%$, thereby allowing flexibility everywhere else. A suitable choice of point is the cycle life has its maximum over SOC_{av} at 100% DOD. This point can be found by partially differentiating the cycle life from Eq. (10) over the SOC_{av} and setting to zero:

$$SOC_{av,100\%,max} = \frac{-s - 100 * u}{2 * v} \tag{11}$$

It is at this maximum point over the SOC that we want the minimum over DOD to occur. Therefore inserting this SOC_av value into Eq. (10) and setting $DOD = 100$:

$$\begin{aligned} r &= -200 * t - u * \frac{-s - 100 * u}{2 * v} \\ &= \frac{u}{2 * v} * (s + 100 * u) - 200 * t \end{aligned} \tag{12}$$

Reinserting into our original fitting function in Eq. (10), gives:

$$\begin{aligned} CL(DOD, SOC_{av}) = q + (\frac{u}{2 * v} * (s + 100 * u) \\ - 200 * t) * DOD + s * SOC_{av} + t * DOD^2 \\ + u * DOD * SOC_{av} + v * SOC_{av}^2 \end{aligned} \tag{13}$$

Recomputing the fit coefficients for this function using least-squares fitting gives the coefficient values listed in Table 2. It results in the function shown in Fig. 2. The only slightly worse R-square value of 0.7634, and slightly improved Root Mean Square Error of 1188 indicates that the imposed constraint does not significantly degrade the quality of fit.

For the fitted coefficient, the proposed function can analytically be shown to produce no partial minimum over DOD within the viable region characterised by the following four criteria:

$$0\% \leq SOC_{av} \leq 100\% \tag{14}$$

$$0\% \leq DOD \leq 100\% \tag{15}$$

$$DOD \leq 2 * SOC_{av} \tag{16}$$

$$DOD \leq 2 * (100 - SOC_{av}) \tag{17}$$

The result is a normalised model that predicts the normalised battery cycle life not just as a function of depth-of-discharge but also taking into account the average state-of-charge over a cycle.

Finally, the function in Eq. (13) can be normalised as follows:

$$nCL(SOC_{av}, DOD) = \frac{CL_4(DOD, SOC_{av})}{CL_4(DOD_{nom}, SOC_{av,nom})} \tag{18}$$

2.3 Verification of Developed Model

To ensure the developed DOD-SOC_{av} cycle life model is in line with expected results, it is compared to the DOD cycle life model based on [13]. Neither this model, nor associated data, was previously used to fit our model. Given difficulties in replicating the model's cycle life results directly using the published coefficients, the original data points are used to refit an exponential function as proposed, against which our model can then be compared. Least-squares fitting finds the model as:

$$CL^+ = i \times exp(j \times DOD) \tag{19}$$

with coefficients i and j having values of 67560 and -0.03223, respectively.

Fig. 3 illustrates the comparison between this previously proposed DOD-only cycle life model and our DOD-SOC_{av} model.

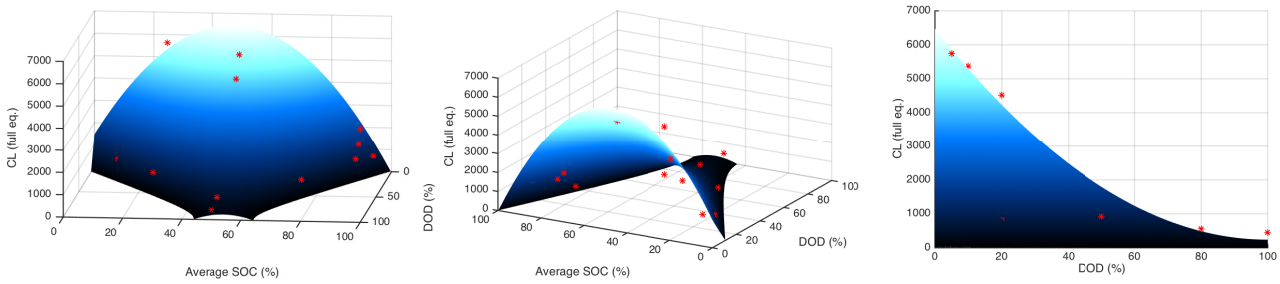

Figure 2: Modified two-variable second-order polynomial fit of cycle life as a function of SOC_{av} and DOD. The figure on far right confirms that local minimum for $DOD < 100$ is no longer visible.

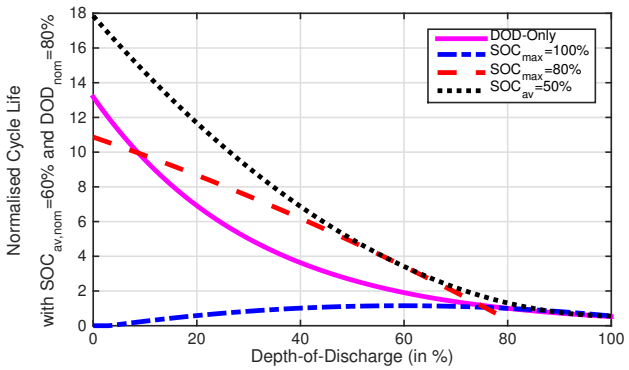

Figure 3: Verification of normalised cycle life models. The DOD-Only model based on [13] does not consider SOC. Our model considers SOC.

The closeness of results depends on both the SOC_av value chosen in our model, as well as the DOD region considered. The curve for $SOC_{max} = 100\%$, which corresponds to the conditions at which the DOD-Only data was collected, is a reasonable fit only above 70% DOD. This is because this choice of SOC represents the boundary case of feasible SOC-DOD behaviour (100% SOC is reached during very cycle) at which curve fitting seems to have its issues. With SOCs away from the edges, either by limiting SOC_{max} to 80%, or by fixing the average SOC to 50%, the resulting curves resemble the previously proposed model notably more closely. Remaining offsets are presumably the result of differences in the battery cells used for the experiments.

Table 3: Parameter limits of data points used for model fitting

Parameter	Minimum value	Maximum value
Temperature	-18°C	40°C
Discharge Current	1C	15C
Charge Current	C/8	4C
Average SOC[a]	10%	95%
DOD[a]	5%	100%

[a] Only part of the SOC-DOD region is feasible; see Eq. 14 - 17.

3. STATIC CASE STUDY: SMARTPHONE

To demonstrate the value of the static cycle life model developed thus far, we illustrate its use on a case study centred around smartphones. One of the suppliers of smartphone battery cells is Panasonic. Its NCA103450 battery, for example, is a prismatic Li-ion cell with a nominal capacity of 2350mAh, almost perfectly matching the 2300mAh offered by the batteries of Google 2013 Nexus 5 smartphone [5, 14]. The cell uses NCA cathodes, similar to those found in Tesla Motors electric vehicles.

Assuming one hour each of calling, browsing, and video watching per day, a new Nexus 5 battery has been shown to last 40 hours [6]. Under this assumption, a user has a wide range of charging options. We consider the following:

1. The battery is charged fully every 24 hours.
2. The battery is charged until full whenever it reaches a state-of-charge of 10%.
3. The battery is charged every 24 hours but only to the optimal level as determined as optimal by our battery ageing algorithm.

The obvious question is: what is the comparative battery life for each of these three charging options?

Using the developed life cycle prediction methodology, finding the answer to this question is quite straightforward. First, the nominal cycle life parameters of the cells need to be considered. The specifications listed in Table 4 are supplied by Panasonic in their associated data sheet [14].

Table 4: Battery cell specifications from Panasonic NCA103450 data sheet

Manufacturer spec	Variable	Value
Nominal capacity (Ah)	N/A	2.35
Nominal cycle life	CL_{nom}	649[a]
Measured at temp (deg C)	T_{nom}	25
Discharge current (C)	$I_{d,nom}$	1
Charging current (C)	$I_{ch,nom}$	0.7
Depth of discharge (%)	DOD_{nom}	100%
Average SOC (%)	SOC_{nom}	50%

[a] The cycle life was determined by digitising the cycle life graph, and linearly scaling forward the degradation seen at 100-500 cycles until the capacity falls below 80% of 2.35Ah.

Table 5: Smartphone cycling scenarios and cycling life outcomes

	Full charge from 10% SOC	Daily full charge	Daily optimal charge
$i_d(C)$	0.025		
$i_{ch}(C)$	0.7		
$T(dC)$	25		
DOD (%)	90	60	
SOC_{av}	55	70	51.09
$CL_{equiv.}$	963	1359	4040
CL_{actual}	1070	2265	6733
Life (years)	4.88	6.20	18.4

Assuming discharging at a steady rate, the current draw during its 40-hour battery life is:

$$I = \frac{2350Ah}{40h} = 58.75mA \tag{20}$$

Or:

$$I = \frac{58.75mA}{2350Ah} = 0.025C \tag{21}$$

The cycle life can then be estimated using our prediction methodology for the three use cases discussed previously, as defined by the parameters as listed in the upper part of Table 5.

As indicated in the final three rows of the table, the predicted cycle lives differ significantly. For the given assumptions, the smartphone battery is predicted to last around six years for daily full charging, versus five years for full charging only whenever 10% SOC is reached. However, an optimal daily charge approach, which is determined as having an average SOC of 51% (i.e. cycling between 21-81% SOC) more than doubles the expected life of the battery.

It should be noted that several of the assumptions mean that the predicted lifetimes are slightly optimistic. These include that battery cells always discharge at a steady rate and continuously operate at exactly $25^{\circ}C$ working temperature. Better tailored assumptions would be likely to allow more accurate cycle life predictions. Nevertheless, it is clear that a strategic charging system has the potential to dramatically increase the expected lifetime of the battery.

4. MODELLING OF DYNAMIC CYCLES

The methodology presented thus far is able to predict the battery lifespan for all scenarios in which an identical charge-discharge cycle is repeated over the full life of the battery. However, in most applications, the cycles change dynamically over time. In electric vehicles, for example, the current input and output needs to change dynamically to provide timely vehicle acceleration and regenerative braking, respectively. And even in less variable application such as energy storage of surplus renewable generation, day-to-day variations in surplus generation lead to a variability in the cycling depth-of-discharge.

4.1 Rainflow Counting

To allow dynamic cycling, we have extended the prediction methodology using an approach called rainflow counting. This process combines a data set with non-uniform fluctuations in at least one variable into numerous data sets of uniform fluctuations by prioritising the most extreme fluctuations and discretising. In effect, rainflow counting screens a series of data for subsequent local maxima and minima indicating local cycle loops. Once found, these loops are recorded and removed from the data until the remaining loops become ever larger. It thereby preserves the most significant peaks and troughs to be considered last. The method is traditionally used for predicting material fatigue but has also been proposed for the prediction of battery ageing (e.g. [12]). In many battery applications such as electric cars with regeneration capability, batteries see notable short-term fluctuations in their state-of-charge, while at the same time following overall charge or discharge profiles. Previous experimental research has shown that deep cycling causes the most significant degradation whereas smaller cycles are

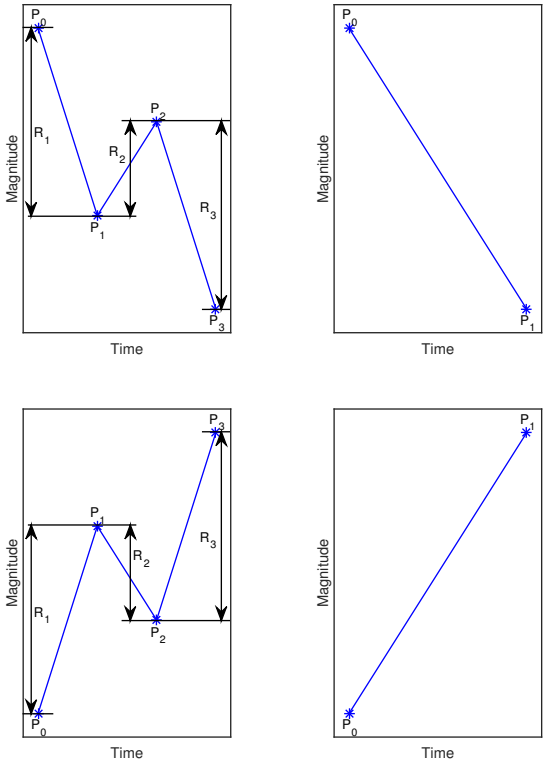

Figure 4: Rainflow counting algorithm illustrated on two profiles. Left and right shows the profiles before and after counting a local cycle, respectively.

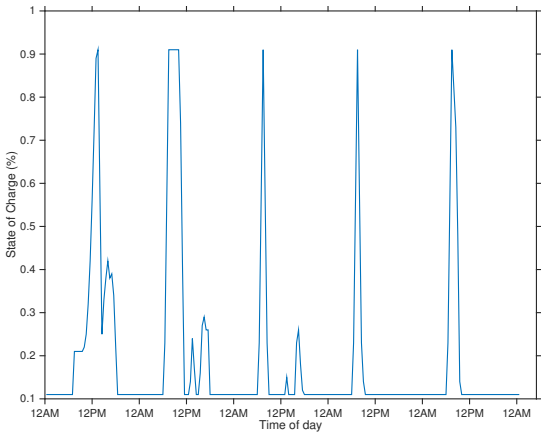

Figure 5: 5-day sample of battery SOC profile. The battery is found to cycle notably between 10% and 90% SOC with some smaller cycles occurring in-between.

less significant (e.g. [4]). As a result, rainflow counting is very suitable for modelling battery ageing.

Rainflow counting can be done in the form of either three- or four-point algorithms, which have been shown to be mathematically identical [8]. The three-point algorithm is faster as it only considers the two cycling ranges existing between three points in each iteration, as apposed to four points and three ranges for the four-point method. However, the three-point method requires an initial prearrangement of the data in order to start at either the global maximum or minimum. This inhibits real-time use of the method. To avoid this limitation, we have opted for the four-point approach.

The four-point rainflow counting method works as follows. It takes as input a set of data containing only the turning points. It then steps through this data from start to end, evaluating four turning points at a time. For each set of four points $P_0, ..., P_3$, three associated ranges are calculated:

$$R_k = |P_k - P_{k-1}| \tag{22}$$

where $k \in 1, 2, 3$. For a given set of four points, a local cycle is identified when the middle range has a smaller magnitude than the two outside ranges:

$$(R_k \geq R_{k-1}) \cap (R_{k-2} \geq R_{k-1}) = 1 \tag{23}$$

Following identification of a local cycle, the associated points P_1 and P_2 are recorded and removed from the dataset, and the algorithm continues. As shown in Fig. 4 this identification and removal approach works both when a local maximum is followed by a local minimum, and vice versa. Once the end of the data set is reached, the remaining cycles are accounted for through sequential repetition of the remaining points and rerunning the algorithm. When the end is reached the second time, all cycles have been accounted for. A more in-depth explanation of the algorithm as well as the pseudocode used as the basis for our programming code can be found in [8].

4.2 Dynamic Cycling Limits

Rainflow counting can be used to deal with variability in individual factor or multiple interlinked factors. An example of two interlinked factors, which we use in the demonstration case study in Section 5, are the maximum and minimum SOC points. As mentioned previously, variability in the depth-of-discharge of a battery is unavoidable for battery systems that are used to support the variable output from renewable generation, e.g. from solar and wind.

4.3 Combining Multiple Independent Factors

If only a single independent variable is considered (such as the temperature, or the charging current), the distribution will be one-dimensional. If multiple independent factors are considered to vary simultaneously, then this can be taken into account by recording not only cycles to be removed but also the other varying factors. Subsequently the cycles are then discretised in further dimensions (one for each varying independent factor), and the ageing map need to be conducted in an equally multi-dimensional form to allow matching up of cycles with corresponding ageing.

5. DYNAMIC CASE STUDY: STORAGE FOR DOMESTIC PV

To illustrate this algorithm, we have chosen to focus on the application of Li-ion battery storage for households that have solar panels. In countries where the feed-in tariff for solar generation has dropped below the typical electricity price, households have incentive to store surplus energy generated for subsequent use. The authors have previously conducted initial simulations to evaluate under which conditions battery storage becomes cost-effective in this context [9]. Here, we will use a randomly-selected simulation profile from the aforementioned paper to demonstrate the proposed ageing model.

5.1 Assumptions

The battery profile considers a $5kWh$ battery installed alongside an Australian household with a $2.5kW_p$ solar panel. The battery operation is optimised from a value-generating perspective that takes into account the electricity and feed-in price, but not the cost associated with battery degradation. It should also be noted that the battery was assumed to be limited to a DOD of 80% as is frequently done to avoid premature battery degradation. A five-day subset of the profile is shown in Fig. 5.

For this case study we have chosen the maximum and minimum state-of-charge to vary dynamically from cycle-

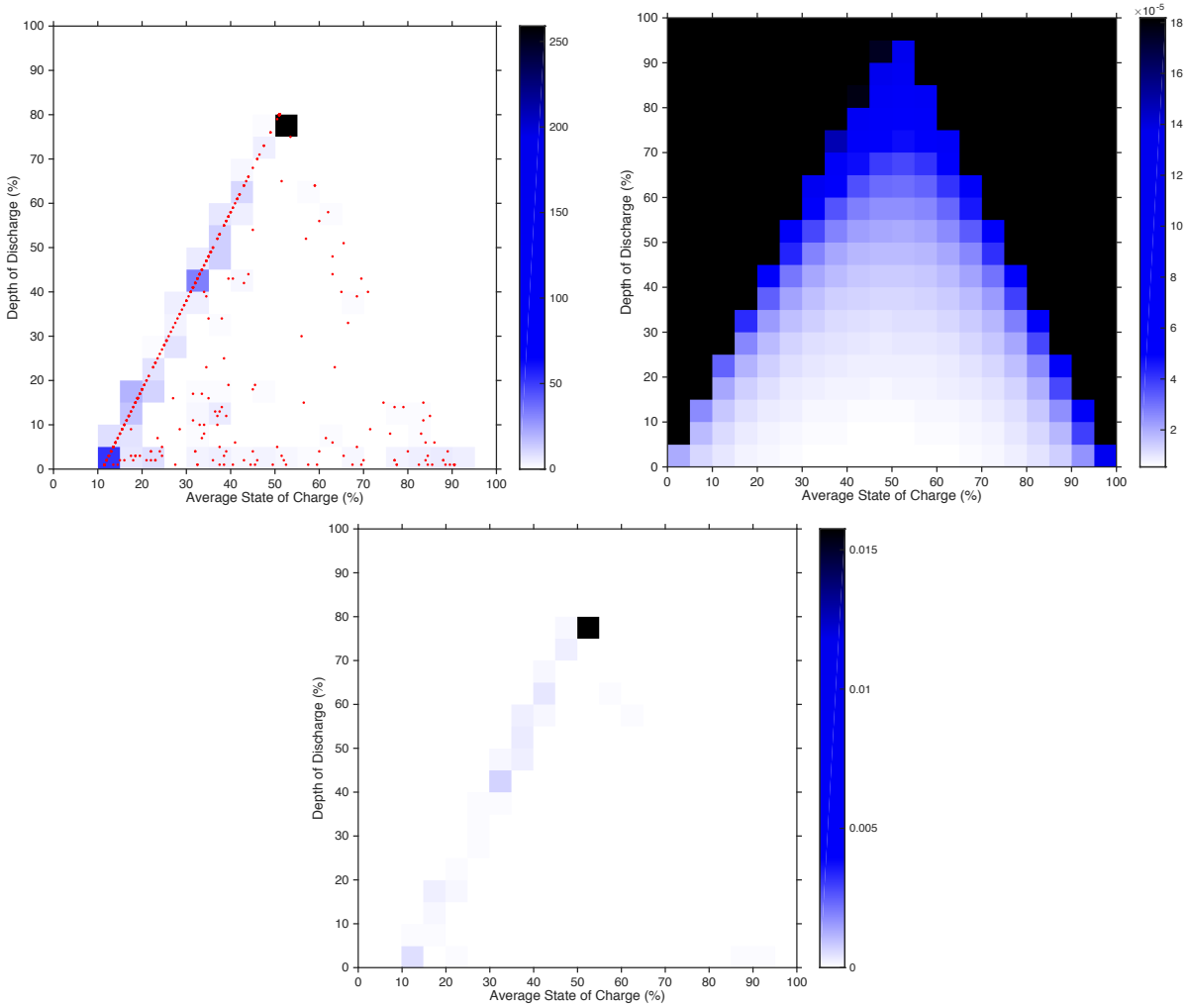

Figure 6: Top left: Cycle distribution after rainflow counting; the points represent individual cycles and the colour map indicates frequency of 5x5% sections. Top right: Fractional battery degradation per cycle for each 5x5% section. Bottom centre: Fractional degradation associated with each section for year-long profile.

Table 6: Domestic PV and storage assumptions. Top: application-specific cycling parameters; bottom: nominal battery parameters.

Battery capacity	5kWh
Operating temperature	25°C
Charge current	0.5C
Discharge current	1C
Maximum SOC	Dynamic (from profile)
Minimum SOC	Dynamic (from profile)
Nominal battery life	1200 cycles
@ Temperature	25°C
@ Charge current	0.5C
@ Discharge current	1C
@ Depth-of-discharge	80%
@ Average SOC	60%

to-cycle. The operating temperature, as well as the charge and discharge currents, are assumed to be fixed and have the values given in Table 6. the turning points fall at the times when the battery current changes direction. That is, the battery transitions either from charging to discharging, or vice versa.

5.2 Cycling Frequency

The first step is extracting the turning points from the data set. Next, the 4-point rainflow counting algorithm described in Section 4.1 is applied. The counted cycles are then discretised into segments, which we have chosen to be 5% SOC_{av} by 5% DOD.

The top left side of Figure 6 illustrates the cycle results. All individual extracted cycles are represented as points, whereas the colour map indicates the frequency of each discretised segment occurring in the one-year profile. It can be seen that by far the most frequent cycle is the maximum allowed battery cycle of 80% DOD and 50% SOC_{av}, corresponding to cycling between the boundaries 10% and 90% SOC.

5.3 Degradation

To calculate degradation, the cycling frequency matrix has to be matched with a matrix containing degradation per cycle for each segment. A matrix of cycle lives is found by evaluating ageing used the methodology presented Section 2 for the assumptions valid for each individual segment. This is converted to a matrix of degradation per cycle with elements D_k as follows:

$$D_k = \frac{1}{CL_k} \tag{24}$$

The resulting degradation map is shown on the top right side of Figure 6. It shows the analogous trend to Figure 2 in that the degradation per cycle increases with both increasing depth-of-discharge and when moving towards either extreme of the state-of-charge region.

The predicted battery degradation for the year-long data set can now be found by multiplying each sector frequency with its related degradation per cycle. This leads to the desired annual degradation matrix illustrated in Figure 6 bottom centre. The resulting degradation trends are similar to the frequency map, which is to be expected as many cycles of one type are likely to cause a notable degradation. By accumulating all points on the map, the total degradation over the year can be found. Assuming the profile is repeated year-after-year and that degradation occurs linearly, this can be used to estimate the lifetime of the battery cells until the capacity has reduced to a specific point. The results for the domestic PV with storage case study are listed in Table 7.

Table 7: Degradation result for storage alongside domestic PV generation

Degradation over one year	2.19%
Lifetime to 70%	13.72 years

6. CONCLUSIONS AND FUTURE WORK

6.1 Conclusions

In this paper we have presented a simple, yet powerful, methodology for predicting battery degradation rates and life spans that takes into account multiple impact factors. The methodology relies on a degree of independence between certain impact factors. For each independent factor, or set of factors, a normalised degradation model is developed based on curve-fitting of experimental data. In the paper this is demonstrated for lithium-ion batteries. The models are subsequently unified and combined with nominal battery information to allow prediction of cycle life under any given set of cycling conditions.

The developed static model was demonstrated on a static case study of a mobile phone. The case study found that daily charging to around 81% state-of-charge can prolong life significantly over both daily charging to 100% or charging fully only when the battery is nearly depleted. This suggests opportunities for charging solutions that improve battery management without requiring any user input or change in behaviour.

The paper further proposes a method to take into account dynamic variations in cycle parameters. A rainflow counting algorithm is used for determining and counting cycles, and discretisation is used to match cycles with degradation rates from our life prediction methodology.

The dynamic method is illustrated via a case study on batteries for households with PV generation. It identifies both the degradation caused by each discretised cycling interval, as well as the collective degradation caused by the applied cycling profile.

The resulting methodology provides a basis for conducting evaluations of battery life and optimisation of battery management for any battery-related applications.

6.2 Further Work

Future work to be done on this model is to extend the validation of the impact factor models against further experimental data. In particular, the individual factor models need to be evaluated for different cell chemistries to ensure suitability. Further factors should also be considered for inclusion in the methodology. One obvious such factor is the impact of resting periods between cycles, which over short times can lead to recovery effects but over long periods must include elements of calendar ageing.

7. ACKNOWLEDGMENTS

The first author would like to thank all members of Penn State University's Control Optimization Laboratory for the many stimulating discussions and collaborative work related to battery ageing, which form the basis on which this work is built. Particular thanks go to Michael Rothenberger and Ji Liu.

8. REFERENCES

[1] M. Broussely, P. Biensan, F. Bonhomme, P. Blanchard, S. Herreyre, K. Nechev, and R. Staniewicz. Main ageing mechanisms in li-ion batteries. *Journal of Power Sources*, 146:90–96, 2005.

[2] N. A. Chaturvedi, R. Klein, J. Christensen, J. Ahmed, and A. Kojic. Algorithms for advanced battery-management systems. *IEEE Control Systems*, 30(3):49–68, 2010.

[3] M. Ecker, J. B. Gerschler, J. Vogel, S. Käbitz, F. Hust, P. Dechent, and D. U. Sauer. Development of a lifetime prediction model for lithium-ion batteries based on extended accelerated aging test data. *Journal of Power Sources*, 215:248–257, 2012.

[4] M. Ecker, N. Nieto, S. Kaebitz, J. Schmalstieg, H. Blanke, A. Warnecke, and D. U. Sauer. Calendar and cycle life study of Li(NiMnCo)O_2-based 18650 lithiumion batteries. *Journal of Power Sources*, 248:839-851, 2014.

[5] Google. Nexus 5. http://www.google.com/nexus/5.

[6] GSMArena. LG Nexus 5 battery life test. http://blog.gsmarena.com/nexus-5-grinds-through-our-battery-test-routine.

[7] Lux Research. Energy storage market rises to $50 billion in 2020, amid dramatic changes. http://www.luxresearchinc.com/news-and-events/press-releases/read/energy-storage-market-rises-50-billion-2020-amid-dramatic.

[8] C. McInnes and P. Meehan. Equivalence of four-point and three-point rainflow cycle counting algorithms. *International Journal of Fatigue*, 30(3):547–559, 2008.

[9] V. Muenzel, J. de Hoog, I. Mareels, A. Vishwanath, S. Kalyanaraman, and A. Gort. PV generation and demand mismatch: Evaluating the potential of residential storage. In *Proceedings of IEEE PES ISGT 2015; in print.*

[10] V. Muenzel, I. Mareels, J. de Hoog, A. Vishwanath, and S. Kalyanaraman. Affordable batteries for green energy are closer than we think. https://theconversation.com/affordable-batteries-for-green-energy-are-closer-than-we-think-28772.

[11] S. S. Ng, Y. Xing, and K. L. Tsui. A naive bayes model for robust remaining useful life prediction of lithium-ion battery. *Applied Energy*, 118:114–123, 2014.

[12] A. Nuhic, T. Terzimehic, T. Soczka-Guth, M. Buchholz, and K. Dietmayer. Health diagnosis and remaining useful life prognostics of lithium-ion batteries using data-driven methods. *Journal of Power Sources*, 239:680–688, 2013.

[13] N. Omar, M. A. Monem, Y. Firouz, J. Salminen, J. Smekens, O. Hegazy, H. Gaulous, G. Mulder, P. Van den Bossche, T. Coosemans, and J. Van Mierlo. Lithium iron phosphate based battery – Assessment of the aging parameters and development of cycle life model. *Applied Energy*, 113:1575–1585, 2014.

[14] Panasonic. NCA103450 data sheet. https://www.master-instruments.com.au/cgi/ajax/get_file/63186/1.

[15] The Boston Consulting Group. Batteries for electric cars: Challenges, opportunities and the outlook to 2020. https://www.bcg.com/documents/file36615.pdf.